Biomechanics of a Fixed–Center of Rotation Cervical Intervertebral Disc Prosthesis

Neil R. Crawford, Seungwon Baek, Anna G.U. Sawa, Sam Safavi-Abbasi, Volker K.H. Sonntag and Neil Duggal

Int J Spine Surg 2012, 6 () 34-42
doi: https://doi.org/10.1016/j.ijsp.2011.10.003
https://www.ijssurgery.com/content/6/34

The International Journal of Spine Surgery
2397 Waterbury Circle, Suite 1,
Aurora, IL 60504, Phone: +1-630-375-1432

Available online at www.sciencedirect.com

SciVerse ScienceDirect

International Journal of Spine Surgery 6 (2012) 34–42

www.sasjournal.com

Biomechanics of a Fixed–Center of Rotation Cervical Intervertebral Disc Prosthesis

Neil R. Crawford, PhD [a,*], Seungwon Baek, MS [a], Anna G.U. Sawa, MS [a], Sam Safavi-Abbasi, MD [b], Volker K.H. Sonntag, MD [a], Neil Duggal, MD [c]

[a] *Spinal Biomechanics Laboratory, Barrow Neurological Institute, Phoenix, AZ*
[b] *Department of Neurosurgery, College of Medicine, University of Oklahoma, Oklahoma City, OK*
[c] *Department of Neurological Surgery, London Health Sciences Centre, London, Ontario, Canada*

Abstract

Background: Past in vitro experiments studying artificial discs have focused on range of motion. It is also important to understand how artificial discs affect other biomechanical parameters, especially alterations to kinematics. The purpose of this in vitro investigation was to quantify how disc replacement with a ball-and-socket disc arthroplasty device (ProDisc-C; Synthes, West Chester, Pennsylvania) alters biomechanics of the spine relative to the normal condition (positive control) and simulated fusion (negative control).

Methods: Specimens were tested in multiple planes by use of pure moments under load control and again in displacement control during flexion-extension with a constant 70-N compressive follower load. Optical markers measured 3-dimensional vertebral motion, and a strain gauge array measured C4-5 facet loads.

Results: Range of motion and lax zone after disc replacement were not significantly different from normal values except during lateral bending, whereas plating significantly reduced motion in all loading modes ($P < .002$). Plating but not disc replacement shifted the location of the axis of rotation anteriorly relative to the intact condition ($P < 0.01$). Coupled axial rotation per degree of lateral bending was 25% ± 48% greater than normal after artificial disc replacement ($P = .05$) but 37% ± 38% less than normal after plating ($P = .002$). Coupled lateral bending per degree of axial rotation was 37% ± 21% less than normal after disc replacement ($P < .001$) and 41% ± 36% less than normal after plating ($P = .001$). Facet loads did not change significantly relative to normal after anterior plating or arthroplasty, except that facet loads were decreased during flexion in both conditions ($P < .03$).

Conclusions: In all parameters studied, deviations from normal biomechanics were less substantial after artificial disc placement than after anterior plating.

Keywords: Artificial disc; Biomechanics; Kinematics

Several experiments have been performed in recent years to study the biomechanics of artificial discs implanted in the cervical spine (summarized by Crawford[1] and Baaj et al.[2]). Most of these experiments have had a narrow focus, studying primarily the effect of devices on the spine's range of motion (ROM). We performed a multifaceted experiment to quantify a number of previously seldom documented experimental parameters characterizing the biomechanics of the cervical spine before and after insertion of a fixed–center of rotation cervical disc prosthesis (ProDisc-C; Synthes, West Chester, Pennsylvania). To our knowledge, no single study has reported an array of parameters as large as was studied here. It was hypothesized that after insertion of the disc prosthesis, there would be only minimal alteration to these biomechanical parameters compared with the intact spine. As a negative control, spines were also studied in the plated condition.

Methods

Ten human cadaveric C3-6 specimens were used (5 male and 5 female cadavers; age range, 37–69 years; mean age, 58 years). Specimens were obtained fresh frozen, thawed in a bath of normal saline solution at 30°C, and carefully cleaned of muscle tissue without damaging any ligaments,

* Corresponding author: Neil R. Crawford, PhD, Spinal Biomechanics Laboratory, Barrow Neurological Institute, 350 W Thomas Rd, Phoenix, AZ 85013; Tel: 602-406-6652; Fax: 602-406-7197.
E-mail address: neil.crawford@chw.edu

2211-4599
10.1016/j.ijsp.2011.10.003

Fig. 1. Posterior photo of specimen showing placement of strain gauge pads on lamina near facet joint. The pads contained 4 uniaxial gauges oriented parallel. The pads were aligned with gauge axes approximately parallel to the predicted primary direction of loading when the facets were compressed.

discs, or joint capsules. Plain film X-rays were taken to verify that specimens had no obvious flaws, especially osteophytes or disc narrowing. For testing, screws were inserted in the exposed endplates and facet articulations, and the heads of the screws were potted in polymethyl methacrylate in metal fixtures.

As has been reported for lumbar spine testing,[3,4] custom arrays of 4 uniaxial strain gauges (Vishay Micro-Measurements, Raleigh, North Carolina) were mounted on the left lamina of C4 near the left C4-5 facet joint (Fig. 1). In 2 of 10 specimens, a second pad was glued to the right C4 lamina for bilateral strain measurements. Gauges were glued to the bone with their axes aligned with the predicted primary strain direction (Fig. 1). After application of gauges, a 1.25-mm-diameter stainless steel guidewire was inserted in the lamina or spinous process of C4 and the electrical leads for the gauges were glued to this wire to serve as "strain relief," ensuring that movement of the spine during testing would not cause any tension in the leads relative to the gauges, which could alter the strain readings.

Specimens were tested nondestructively in the intact condition, again after insertion of the disc prosthesis at C4-5, and again after simulated fusion across C4-5 with an anterior locking plate. Surgical procedures were performed with the specimens upright on the testing apparatus to maintain the same optical marker calibration in each condition.

The disc prosthesis was available in 5-, 6-, and 7-mm heights and with medium, large, and extra-large footprints; the appropriate size was chosen based on the anatomy of each specimen. Of the specimens, 9 required 5-mm devices and 1 required a 6-mm device; all 10 specimens used a medium footprint. The prosthesis was implanted with the manufacturer's recommended tools, although procedures were performed with the specimen positioned upright. In brief, a discectomy was performed, and the posterior longitudinal ligament was resected. The endplates were flattened with a curette and a high-speed drill (The Anspach Effort, Palm Beach Gardens, Florida). Slots to receive the device's keels were cut with a cutting chisel. The device was then attached as a single unit to the insertion tool and driven into place with a hammer.

After removal of the disc prosthesis, no further preparation of the disc space was performed before insertion of a wedge graft (polyetheretherketone; Synthes) and application of a locking plate (Cervical Spine Locking Plate; Synthes). Wedge grafts were available in heights to match the height of the disc prosthesis. Plates were available in 14-, 16-, and 18-mm lengths. Of the specimens, 4 used 14-mm plates, 2 used 16-mm plates, and 4 used 18-mm plates. In all specimens 4.0 × 14–mm titanium screws were used to attach plates.

In both intact and instrumented conditions, specimens were studied sequentially in 2 different loading apparatuses. First, for pure moment flexibility testing, an apparatus was used in which a system of cables and pulleys imparts nondestructive, nonconstraining torques in conjunction with a standard servohydraulic test system (858 Mini Bionix; MTS Test Systems, Minneapolis, Minnesota), as described previously[5] (Fig. 2A). This technique gives reproducible results because a pure moment is distributed uniformly across the specimen regardless of the point of load application.[6] Loads were applied about the appropriate anatomic axes to induce 3 different types of motion: flexion-extension, left and right lateral bending, and left and right axial rotation. Applied cable force was monitored from a uniaxial load cell in line with the piston of the servohydraulic test frame and converted to applied moment based on the radius of the pulley attached to the specimen. In each direction of loading, before data collection, the specimen was preconditioned 3 times to 1.5 Nm for 60 seconds. After the third preconditioning cycle, the specimen was allowed to recoil for 60 seconds with no load before data collection. During the data collection cycle, loads were applied in a quasistatic manner in 0.25-Nm increments to a maximum of 1.5 Nm.

Next, for more physiological flexion-extension loading modeling the natural vertical compression from head weight and muscular co-contraction, the specimens were transferred to a compression-flexion apparatus (Fig. 2B). In this apparatus, movement was induced until specimens reached the same C3-6 angle (sum of C3-4, C4-5, and C5-6 angles) that was previously achieved during pure moment flexibility tests for that condition. The rationale behind targeting, with this more complex load, the same angle that was reached with the simple (pure moment) load is that equivalent "muscular exertion" is likely created in both apparatuses; the alternative, using some measurement of applied load or combination of torques and forces in a load-controlled experiment, is ambiguous and difficult.

Three-dimensional specimen motion in response to the applied loads during pure moment and compression-flexion

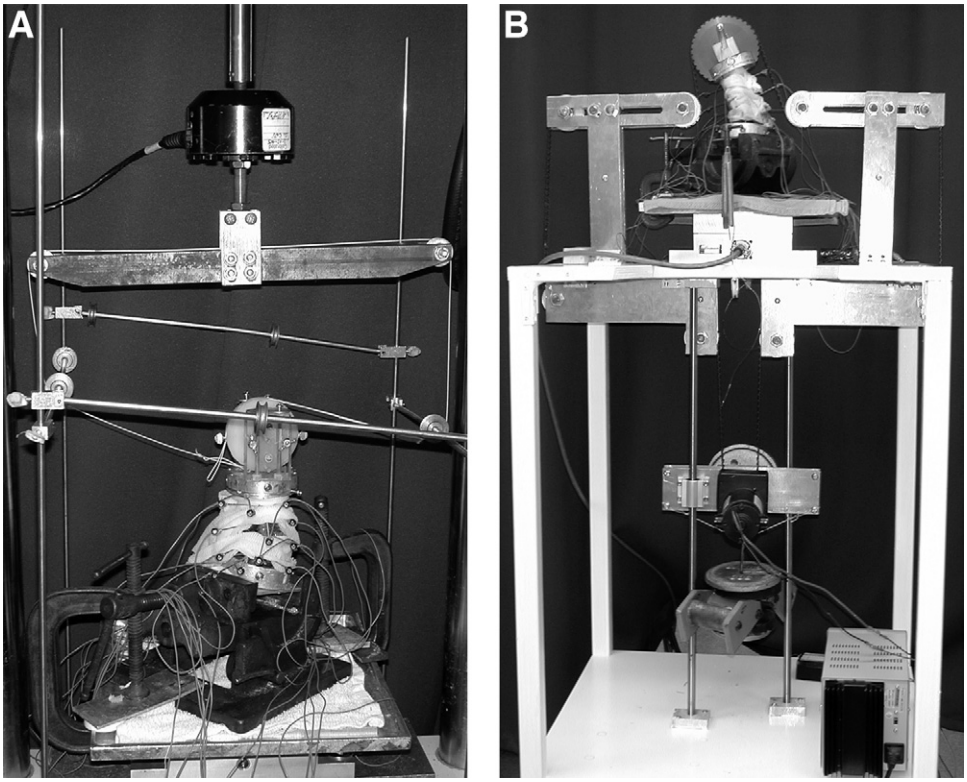

Fig. 2. Specimen loading configurations. (A) Photo from a right-side perspective of a pure moment flexibility test. Strings and pulleys in conjunction with a standard servohydraulic test frame were used to induce flexion (shown), extension, axial rotation, and lateral bending. (B) Photo from a left-side perspective of a flexion-compression test. An electric motor connected to the upper fixture with a heavy-duty belt induced flexion or extension. Weights hung from the motor applied a constant compressive follower load of 70 N. Because of the orientation of the pulleys, the direction of the follower load stayed aligned with the axis of the specimen throughout movement.

tests was determined with the Optotrak 3020 system (Northern Digital, Waterloo, Ontario, Canada). This system measures the 3-dimensional displacement of infrared-emitting markers rigidly attached in a noncollinear arrangement to each vertebra in a stereophotogrammetric manner (Fig. 2). Custom software collected optical tracking and applied load data at 2 Hz (quasistatic tests) or 60 Hz (compression-flexion tests) and converted the marker coordinates to angles about each of the anatomic axes in terms of the motion segment's coordinate system.[7] Spinal angles were calculated with a technique that provides the most appropriate results for describing the spine's angular coupling patterns.[8] During both pure moment and compression-flexion tests, a separate computer measured and recorded voltages across the strain gauges at 10 Hz synchronously with data collected from the optical tracking and applied load measurement systems.

Testing for 1 specimen required 1 or 2 days. If a second day of testing was needed, specimens were refrigerated overnight to mitigate degradation. Refreezing of specimens was avoided for fear of damaging the bone–strain gauge interface. After completion of all testing, the C4-5 level was disarticulated by transecting the disc and facet regions with a scalpel, and the strain gauges were calibrated by applying test loads of known magnitude over a grid of 8 to 32 locations by use of a small plunger oriented normal to the C4 facet surface (Fig. 3). By use of these test loads, independent neural network models were built and trained for each specimen with Predict software (Neuralware, Carnegie, Pennsylvania), enabling identification of the location and magnitude of forces transferred by the facets during the experiment based on the strain recordings that were taken during pure moment and compression-flexion tests.[3] As a check of accuracy of calculated facet loads, additional point loads applied at different locations not used for training the neural network model were recorded in disarticulated specimens and compared with calculated values.

From the raw data, several parameters were calculated. The angular ROM during motion in all planes, angular lax zone (LZ) (portion of ROM in which ligaments and hardware are lax), and stiff zone (SZ) (portion of ROM in which ligaments and hardware are under tension) were determined from flexibility tests.[9] ROM is the angle reached at 1.5 Nm. The boundary between LZ and SZ is the displacement where a line through the upper SZ (0.75, 1.0, 1.25, and 1.5 Nm and their corresponding angles) is extrapolated to zero load. LZ and SZ sum to form the ROM. The neutral position is, by definition, the angle halfway between the positive LZ/SZ boundary and the negative LZ/SZ boundary. In ad-

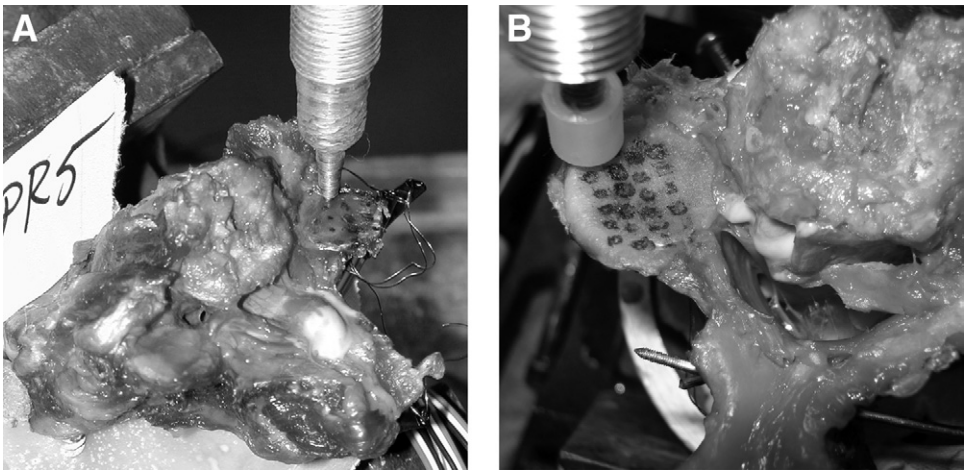

Fig. 3. Calibration of strain gauges required the specimen to be disarticulated after completion of testing. Then, test loads were applied with the MTS piston fitted with a plunger. Loads were applied to a series of points (shown marked with permanent ink) while output from each strain gauge was recorded. A neural network model used these test loads to establish the relationship between strain gauges and facet load. (A) In the first 6 specimens, a metal plunger with a small tip was used. (B) In the last 4 specimens, a rounded plastic plunger was used, which provided a surface mimicking the opposing facet better than the metal plunger.

dition, from flexibility tests, the angular coupling ratio, defined as the coupled angle (relative to neutral position) under full load divided by the primary angle under full load, was determined. Facet loads from strain gauges during loading in each direction were also determined from calibrated strain data.

The location of the instantaneous axis of rotation (IAR) during flexion and extension with follower load was determined in the midsagittal plane in a centrode of 1.0° increments. This centrode was then averaged to find the mean position of the IAR across full range. The IAR was assumed to be equivalent to the finite helical axis of motion (ignoring translation along the axis) determined from marker data with methods described by Spoor and Veldpaus.[10] Before calculating IARs, we smoothed the xyz position data files using a moving average of ±10 frames of data (smoothed frame represents average over 21 frames). This smoothing algorithm greatly reduced noise but had little effect on IAR position because movement was relatively slow (approximately 1° per second) and the data capture rate was relatively fast (approximately 60 frames per second). After smoothing, an iterative algorithm was used to determine the next frame satisfying the requirement of a greater than 1.0° difference from the previously selected frame. As described elsewhere,[11] IARs were overlaid on roughly approximated anatomic images that were scaled according to known anterior, posterior, and middle landmarks that had been used for establishing local coordinate systems.

All data were statistically analyzed by 1-way repeated-measures analysis of variance followed by Holm–Sidak tests to determine whether outcome measures were significantly different between the intact condition after insertion of the disc prosthesis and after plating. $P < .05$ was considered significant.

Results

ROM, LZ, and SZ

Mean angular ROM and LZ at C4-5 after arthroplasty matched intact values well during flexion and extension (Fig. 4, Table 1). During lateral bending, ROM was reduced to 70% of intact and LZ was reduced to 50% of intact. During axial rotation, LZ was reduced to 67% of intact.

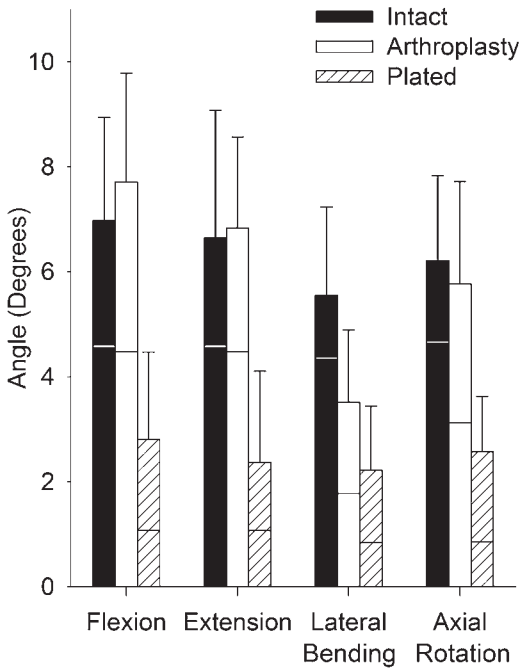

Fig. 4. Mean angular motion in each condition studied. Full bars represent ROM; the portion below the horizontal line represents LZ, and the portion above the horizontal line represents SZ. Error bars show standard deviation of ROM.

Table 1
Mean angular ROM, LZ, and SZ

Parameter and loading mode	Normal (mean ± SD) (°)	Arthroplasty (mean ± SD) (°)	Plated (mean ± SD) (°)
ROM			
Flexion	7.0 ± 1.6*	7.8 ± 1.9*	3.2 ± 2.3
Extension	6.9 ± 1.9*	6.7 ± 1.9*	2.9 ± 2.0
Lateral bending	5.4 ± 1.6*	3.8 ± 1.3*†	2.6 ± 1.5
Axial rotation	6.1 ± 1.4*	5.7 ± 1.6*	3.0 ± 1.4
LZ			
Flexion-extension	9.5 ± 2.8*	9.7 ± 3.6*	2.9 ± 3.2
Lateral bending	8.4 ± 2.9*	4.2 ± 2.0†	2.3 ± 2.1
Axial rotation	9.1 ± 2.2*	6.1 ± 2.4*†	2.5 ± 2.3
SZ			
Flexion	2.2 ± 0.5	2.9 ± 0.9*	1.7 ± 0.9
Extension	2.2 ± 0.6	1.9 ± 0.9	1.4 ± 0.6
Lateral bending	1.2 ± 0.2	1.7 ± 0.5†	1.4 ± 0.6
Axial rotation	1.5 ± 0.4	2.6 ± 0.8*†	1.7 ± 0.4

* Significantly different from plated.
† Significantly different than intact.

These reductions were statistically significant ($P < .010$) (Table 1). The plated condition allowed significantly less ROM or LZ in all loading directions than the intact condition. The plated condition also allowed significantly less ROM in all loading directions and less LZ in flexion-extension and axial rotation than the arthroplasty condition.

Mean angular SZ at C4-5 after arthroplasty was greater than the intact SZ during extension, lateral bending, and axial rotation (Fig. 4, Table 1). These increases were statistically significant during lateral bending and axial rotation ($P < .001$). During extension, SZ was 98% of intact. The plated condition allowed an SZ that was not significantly different from intact during any directions of loading ($P > .08$).

Angular coupling

The coupling between axial rotation and lateral bending was strong at C4-5. In intact specimens 0.70° of coupled axial rotation was observed per degree of primary lateral bending (Fig. 5) and 0.55° of coupled lateral bending was observed per degree of primary axial rotation (Fig. 5). With plating, both of these coupled motions were reduced relative to intact, and both of these reductions were statistically significant ($P < .002$). With arthroplasty, coupled axial rotation per degree of lateral bending increased slightly relative to intact ($P = .149$) whereas coupled lateral bending during axial rotation decreased notably relative to the intact condition ($P = .002$).

Sagittal axis of rotation

After arthroplasty, the mean centrode of the axis of rotation through the midsagittal plane at C4-C5 (index level) during flexion to extension with simultaneous follower load shifted significantly rostrally from its intact position ($P = .027$) but did not shift anteroposteriorly ($P = .73$) (Fig. 6). After anterior plating, the sagittal axis of

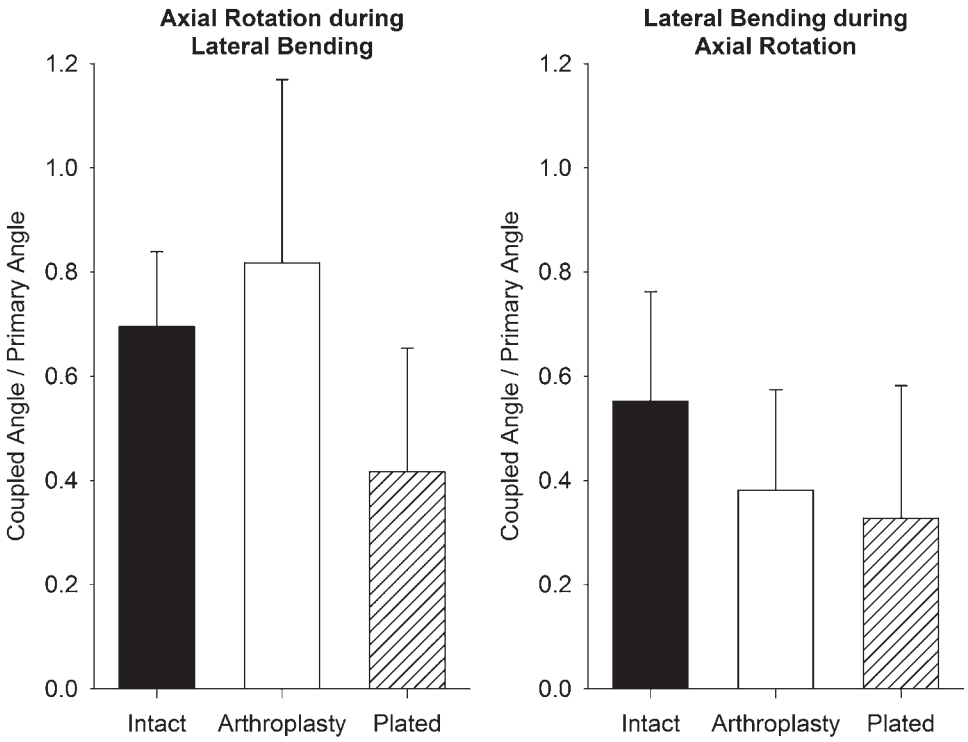

Fig. 5. Angular coupled rotation per degree of primary rotation at C4-5 showing coupling pattern between lateral bending and axial rotation. Error bars show standard deviation.

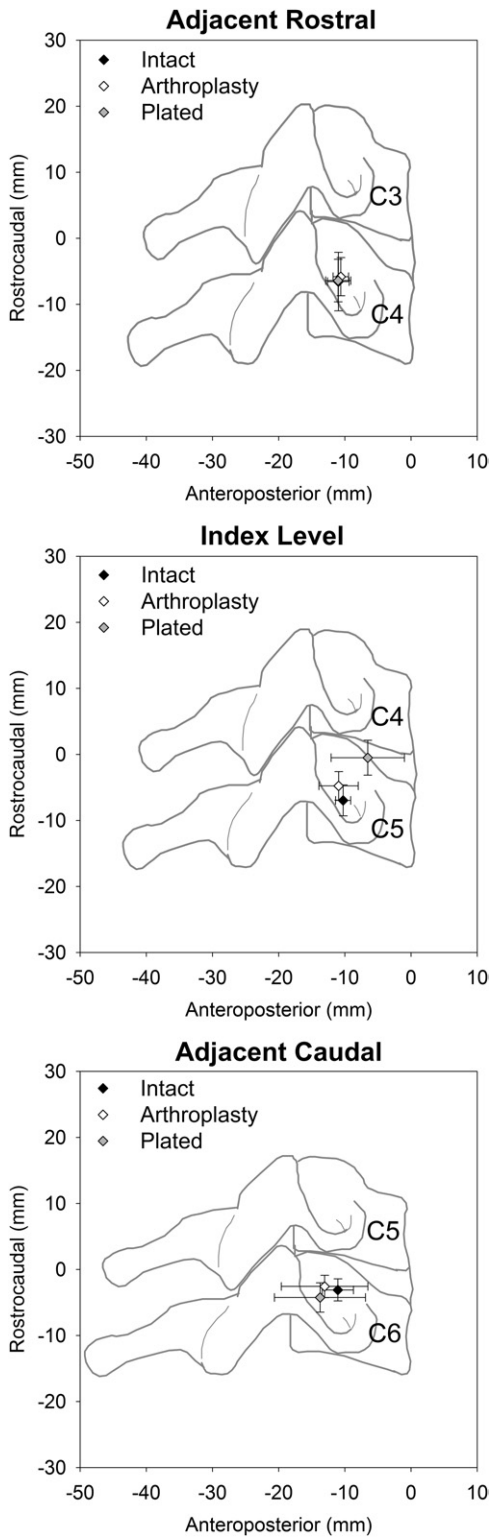

Fig. 6. Mean location of axis of rotation in sagittal plane during flexion to extension at index (C4-5) and adjacent (C3-4 and C5-6) levels. Error bars show standard deviation.

rotation at C4-5 shifted to a position that was both significantly more rostral ($P = .001$) and anterior ($P = .001$) than intact. After both anterior plating and disc replacement, a slight (<1.5 mm) but significant rostral shift in the position of the axis of rotation was found at the adjacent rostral level ($P < .05$); no change in position of the axis of rotation was found at the adjacent caudal level ($P > .19$).

Facet loads

Because data in initial specimens using the metal plunger for calibration (Fig. 3A) were considered inaccurate, the facet load data that were analyzed were limited to the last 4 specimens and a total of 5 facets, which were calibrated with the larger-diameter rounded plastic plunger (Fig. 3B). The mean facet load did not significantly change after arthroplasty or plating, except during flexion with a 70-N follower load, where the mean facet load significantly decreased from intact with either implant system ($P < .03$) (Fig. 7). For intact specimens, there was a significantly greater load on the contralateral facet during axial rotation compared with load on the ipsilateral facet ($P < .03$). This difference was not seen after arthroplasty ($P > .2$) or plating ($P > .9$). The addition of a compressive follower load did not change the magnitude of the facet load during flexion or extension for any condition ($P > .2$).

On the basis of computational models created for a total of 5 facets (using the last 4 specimens), the root-mean-square deviations involved in predicting known loads applied during the calibration procedure were 11.7 N (at 75 N), 8.2 N (at 50 N), 8.7 N (at 25 N), and 7.0 N (at 5.0 N). Similarly, the root-mean-square deviations for the load location points (x- and y-components) were below 0.6 linear units (corresponding to approximately 1.5 mm). This level of error is reasonably low, lending additional confidence in the facet load computation method.

Discussion

ROM, LZ, and SZ

With regard to flexion and extension (sagittal-plane motion), the angular ROM after arthroplasty matched the intact

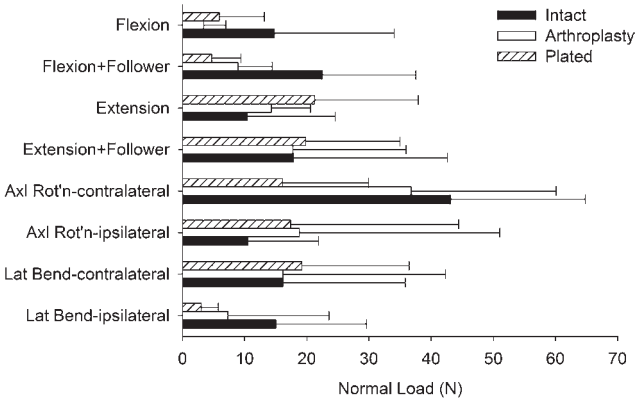

Fig. 7. Mean facet loads during different conditions of specimen loading. Facet loads during flexion and extension are averages of right and left sides. Error bars show standard deviation. (Axl Rot'n, axial rotation; Lat Bend, lateral bending.)

values well at the index level ($P > .3$) (Fig. 4). Similarly, the angular LZ and SZ also matched intact values well at the index level ($P > .08$). These findings suggest that the physiological quantity of sagittal cervical motion as defined by the intact spine is well maintained by the arthroplasty device.

With regard to lateral bending (coronal-plane motion), the angular ROM was reduced to 70% of intact after arthroplasty ($P = .01$). Despite this reduction in ROM, the SZ component of the ROM actually increased to 142% of intact ($P = .001$). The significant decrease in the LZ component of the ROM to 50% of intact ($P = .001$) overcame the increase in the SZ component to lead to the net decrease in ROM. This behavior indicates that after arthroplasty, the earliest resistance to coronal-plane motion was met closer to upright than it had been met in the intact condition. However, as motion proceeded, the resistance to further motion was more gradual than it had been in the intact condition. Such behavior may be related to the immediate postoperative condition of specimens and could change with healing in vivo as surrounding tissues become less compliant, although further study would be needed to verify this hypothesis. If this behavior persisted postoperatively, it could be a beneficial property clinically if additional lateral bending stability is needed at the index level because the instrumented level would preferentially remain closer to upright during low–impact activities within the LZ.

With regard to axial rotation (transverse-plane motion), the angular ROM after arthroplasty matched the intact ROM well ($P = .53$). However, although there was no change in the ROM, the SZ component of the ROM increased to 173% of intact ($P = .001$). The significant decrease in the LZ component of the ROM to 67% of intact ($P = .006$) overcame the increase in the SZ component, leading to no net change in ROM. As with lateral bending, this behavior indicates that after arthroplasty, the earliest resistance to transverse-plane motion was met closer to neutral than it had been met in the intact condition. However, as motion proceeded, the resistance to further motion was more gradual than it had been in the intact condition. Such behavior could be related to the testing of specimens in the immediate postoperative condition, where surrounding ligaments were damaged and were more compliant, but the height added by the arthroplasty device placed the remaining ligaments under greater tension. This biomechanical behavior could be potentially beneficial clinically if the goal is to protect the index level, because that level would have greater stability in the lax region near neutral rotation, meaning that the adjacent levels would preferentially move first during low-impact activities.

As expected, plating reduced ROM and LZ in all directions of loading relative to intact and arthroplasty by significant amounts in almost all comparisons (Table 1). However, the SZ, though consistently reduced relative to arthroplasty, was not always reduced relative to intact and was not significantly different from intact in any comparison. This behavior indicates that the elastic behavior of the bone-screw, screw-plate, and bone-plate interfaces while undergoing physiological-range loading is similar to that of the replaced joint. It should be noted that the condition studied is the immediate postoperative condition and it would be expected that, after fusion occurred in actual patients, the elastic response would become stiffer.

ROM data from our study can be compared with data presented by other authors. Three other single-level in vitro studies have been published using the same ball-and-socket cervical arthroplasty device. Chang et al.[12] studied changes in ROM in the cervical spine after insertion of ball-and-socket arthroplasty (using the same total disc replacement [TDR] device as the current study), ball–in–trough arthroplasty, or anterior plating. Motion at C6-7 (and adjacent levels) was studied during application of 2-Nm pure moments with a simultaneous 100-N compressive follower load. In contrast to our study, they found significant increases in ROM at the operated level during flexion and extension after ball-and-socket arthroplasty and insignificant increases in ROM during lateral bending and axial rotation. Similar to our study, they found that plating caused decreased ROM, as expected. It is possible that the different findings that ROM increased instead of decreased during lateral bending and axial rotation are related to differences in test methods, such as the use of pure moment together with compressive follower loads applied through lateral cables instead of pure moment alone, the study of C6-7 instead of C4-5, and the unreported, possibly older, age of cadaveric specimens. It is also unspecified whether the posterior longitudinal ligament was resected, as in our study, or left intact. DiAngelo et al.[13] also studied the same TDR device in cadaveric specimens using applied loads mimicking physiological load patterns. They found insignificant increases in ROM during flexion, lateral bending, and axial rotation and a significant decrease in ROM during extension with the TDR device. Differences from our findings are likely the result of the dissimilar methods of load application. Puttlitz et al.[14] also used pure moments, though to a lower maximum (1.0 Nm), in studying the same cervical TDR device. In closer agreement with our findings than the other published studies, they observed that disc replacement increased ROM to 149% of intact during flexion-extension, decreased ROM to 63% of intact during lateral bending, and decreased ROM to 73% of intact during axial rotation.

Angular coupling

It is known that, in the human cervical spine, there is normally a pattern of strong coupling between lateral bending and axial rotation such that coupled lateral bending occurs simultaneously during axial rotation and, similarly, coupled axial rotation occurs simultaneously during lateral bending.[15,16]

It was found in this experiment that the pattern of coupled axial rotation occurring during lateral bending was maintained fairly close to intact after arthroplasty ($P = .15$)

whereas this pattern was altered after plating ($P = .002$) (Fig. 5). However, the coupling pattern of lateral bending occurring during axial rotation was lost both after arthroplasty ($P = .002$) and after plating ($P = .001$). It is unclear from the design of the device why arthroplasty-implanted spines would match intact kinematics better during lateral bending than during axial rotation. It is also interesting that the opposite was true regarding ROM: arthroplasty-implanted spines matched intact ROM better during axial rotation than during lateral bending.

Puttlitz et al.[14] also measured the coupling pattern with and without cervical disc arthroplasty using the same prosthesis used in our study. As in our study, they measured coupled lateral bending occurring during primary axial rotation, as well as the coupled axial rotation occurring during primary lateral bending. Although they found no significant differences between intact and disc-replaced conditions with regard to the amount of coupling present, they showed that arthroplasty maintained closer agreement with the intact condition in the case of coupled axial rotation during lateral bending than in the case of coupled lateral bending during axial rotation. Similar to our findings, they showed that the coupled lateral bending during axial rotation was somewhat decreased after disc replacement relative to the intact coupling pattern. Coupling after plating was not studied.

Table 2
Summary of alterations relative to intact condition observed for arthroplasty-implanted and plated conditions

Parameter	Arthroplasty	Plated
ROM		
Flexion	No change	Substantial decrease
Extension	No change	Substantial decrease
Lateral bending	Mild decrease	Substantial decrease
Axial rotation	No change	Substantial decrease
LZ		
Flexion-extension	No change	Substantial decrease
Lateral bending	Mild decrease	Substantial decrease
Axial rotation	Mild decrease	Substantial decrease
SZ		
Flexion	No change	No change
Extension	No change	No change
Lateral bending	Mild increase	No change
Axial rotation	Mild increase	No change
Coupled axial rotation during lateral bending	No change	Substantial decrease
Coupled lateral bending during axial rotation	Substantial decrease	Substantial decrease
Anteroposterior position of axis of rotation	No change	Substantial increase
Rostrocaudal position of axis of rotation	Mild increase	Substantial increase
Facet load during flexion	Mild decrease	Mild decrease
Facet load during other loading	No change	No change

Axis of rotation

It was found that although arthroplasty did not affect the anteroposterior position of the axis of rotation during flexion-extension ($P = .727$) (Fig. 6), it shifted the rostrocaudal position of the axis of rotation slightly but significantly rostrally ($P = .027$). Anteroposterior position of the axis of rotation is highly dependent on depth of insertion of the device, and the agreement between arthroplasty-inserted and intact conditions indicates that insertion depth was well chosen on average. The rostrocaudal disagreement in position may not be meaningful, considering that the adjacent rostral segment (C3-4) also showed a rostral shift in axis of rotation relative to intact after arthroplasty or plating. However, this finding may indicate that the motion segment angulated slightly more sharply after arthroplasty than it had done normally.

Facet loads

Because of the change in protocol during facet load assessment (adoption of larger plunger for application of calibration loads) (Fig. 3), facet load data were only available from 5 facets (4 specimens), making meaningful statistical analyses difficult. However, on the basis of the limited data, neither arthroplasty nor anterior plating seemed to affect load distribution through the facets compared with intact during pure moment loading. The significantly decreased facet loads seen with the implants in place (both after arthroplasty and after anterior plating) compared with intact during flexion with a compressive follower load indicate a shift in the distribution of axial compressive loads along the spine during this direction of loading, with the resultant load axis presumably acting more anteriorly. It is unknown what the clinical consequences of this shift in load transfer would be. The data also suggest that changes in kinematic parameters such as ROM caused by implants do not necessarily correlate with changes in load distribution patterns. However, more data are necessary before further conclusions can be drawn.

Similar to us, Chang et al.[17] used strain gauges to measure facet loads after artificial disc insertion. However, they applied only a single strain gauge to the lamina for measuring facet loads. Such a technique is unvalidated and would be expected only to provide a rough approximation of facet load that is heavily dependent on positioning of the strain gauge.

Conclusions

The arthroplasty and anterior plating both altered cervical biomechanics, though in different ways (Table 2). In general, deviations from intact were less substantial after artificial disc placement than after plating. This information extends the understanding of how arthroplasty behaves and aids in comparing the particular device studied with other artificial discs.

References

1. Crawford NR. Analysis: in vitro biomechanical construct tests evaluating cervical arthroplasty. *World Spine J* 2006;1:7–13.
2. Baaj AA, Uribe JS, Vale FL, et al. History of cervical disc arthroplasty. *Neurosurg Focus* 2009;27:E10.
3. Sawa AG, Crawford NR. The use of surface strain data and a neural networks solution method to determine lumbar facet joint loads during in vitro spine testing. *J Biomech* 2008;41:2647–53.
4. Lazaro BC, Brasiliense LB, Sawa AG, et al. Biomechanics of a novel minimally invasive lumbar interspinous spacer: effects on kinematics, facet loads, and foramen height. *Neurosurgery* 2010;66:126–32.
5. Crawford NR, Brantley AG, Dickman CA, Koeneman EJ. An apparatus for applying pure nonconstraining moments to spine segments in vitro. *Spine (Phila Pa 1976)* 1995;20:2097–100.
6. Panjabi MM. Biomechanical evaluation of spinal fixation devices: I. A conceptual framework. *Spine (Phila Pa 1976)* 1988;13:1129–34.
7. Crawford NR, Dickman CA. Construction of local vertebral coordinate systems using a digitizing probe. Technical note. *Spine (Phila Pa 1976)* 1997;22:559–63.
8. Crawford NR, Yamaguchi GT, Dickman CA. A new technique for determining 3-D joint angles: the tilt/twist method. *Clin Biomech (Bristol, Avon)* 1999;14:153–65.
9. Crawford NR, Peles JD, Dickman CA. The spinal lax zone and neutral zone: measurement techniques and parameter comparisons. *J Spinal Disord* 1998;11:416–29.
10. Spoor CW, Veldpaus FE. Rigid body motion calculated from spatial co-ordinates of markers. *J Biomech* 1980;13:391–3.
11. Crawford NR. Technical note: determining and displaying the instantaneous axis of rotation of the spine. *World Spine J* 2006;1:53–6.
12. Chang UK, Kim DH, Lee MC, Willenberg R, Kim SH, Lim J. Range of motion change after cervical arthroplasty with ProDisc-C and Prestige artificial discs compared with anterior cervical discectomy and fusion. *J Neurosurg Spine* 2007;7:40–6.
13. DiAngelo DJ, Foley KT, Morrow BR, et al. In vitro biomechanics of cervical disc arthroplasty with the ProDisc-C total disc implant. *Neurosurg Focus* 2004;17:E7.
14. Puttlitz CM, Rousseau MA, Xu Z, Hu S, Tay BK, Lotz JC. Intervertebral disc replacement maintains cervical spine kinetics. *Spine (Phila Pa 1976)* 2004;29:2809–14.
15. Cook C, Hegedus E, Showalter C, Sizer PS. Coupling behavior of the cervical spine: a systematic review of the literature. *J Manipulative Physiol Ther* 2006;29:570–5.
16. Senouci M, FitzPatrick D, Quinlan JF, Mullett H, Coffey L, McCormack D. Quantification of the coupled motion that occurs with axial rotation and lateral bending of the head-neck complex: an experimental examination. *Proc Inst Mech Eng H* 2007;221:913–9.
17. Chang UK, Kim DH, Lee MC, Willenberg R, Kim SH, Lim J. Changes in adjacent-level disc pressure and facet joint force after cervical arthroplasty compared with cervical discectomy and fusion. *J Neurosurg Spine* 2007;7:33–9.